Proceedings of PVP2007
2007 ASME Pressure Vessels and Piping Division Conference
July 22-26, 2007, San Antonio, Texas

PVP2007-26533

EFFECT OF HYDROGEN GAS PRESSURE ON THE MECHANICAL PROPERTIES OF LOW ALLOY STEEL FOR HYDROGEN PRESSURE VESSELS

Yoru WADA / The Japan Steel Works,LTD **Ryoji ISHIGAKI / The Japan Steel Works,LTD**

Yasuhiko TANAKA / The Japan Steel Works,LTD **Tadao IWADATE / The Japan Steel Works,LTD** **Keizo OHNISHI / The Japan Steel Works,LTD**

ABSTRACT

To provide engineering data useful in design, manufacture and operation of hydrogen storage vessels in hydrogen refueling stations, fatigue test machine equipped with high-pressure hydrogen autoclave was introduced. The effect of steel's strength level, temperature effect, fracture toughness and pressure effect were evaluated in gaseous hydrogen environment. When steel's strength level exceeds around 930MPa to 1000MPa, the elongation and notch tensile properties deleteriously degraded. The elongation reduction by the effect of hydrogen increased with lowering the temperature. The same sensitivity to temperature on crack growth behavior was observed. However, it was shown that the gaseous hydrogen environment only affect the slow stable crack growth but did not affect the critical flaw growth of the steel at low temperature, i.e. fast fracture. The pressure dependence of notch tensile strength ranging from 0.1MPa to 75MPa hydrogen pressure shows approximately 1/2 power dependence.

INTRODUCTION

For the safe use of fuel cell cars, the Japanese government and industry are now going over the regulations and recommended practices for the utilization of hydrogen gas. Since many metal materials will be applied in hydrogen fuel station, it is necessary to establish the appropriate design, manufacturing practice and inspection planning considering material performance under high-pressure hydrogen environment. Since hydrogen fuel stations in Japan are now designed to supply 35MPa high-pressure hydrogen to fuel cell vehicles, the storage pressure might be higher than 35MPa and thus components must withstand under 45MPa (or more higher) hydrogen gas environment. In case of high strength, low alloy steel, it had been recognized that external hydrogen gas would cause severe hydrogen embrittlement. Ohnishi [1] surveyed hydrogen embrittlement of AISI 4340 steel in ambient gaseous hydrogen and presented that hydrogen cracking occurs with almost "no incubation time". During 1960-1970's, several researchers identified such characteristic behaviors in gaseous hydrogen [2] [3] [4], and this phenomenon is denoted "hydrogen environment embrittlement(H.E.E.)" as distinguished from the embrittlement of hydrogen charged steel [5]. A lot of work supports the fact that H.E.E. occurs after the steel (or metal) is subjected to the plastic deformation. This is considered because crack initiation is associated with hydrogen adsorption and absorption process at the fresh metal surface breaking the oxide barrier. It is also well known that the impurity gases such as oxygen significantly interfere hydrogen embrittling process at the crack tip even in ppm level [2] [6]. Knowing that such characteristic behavior in gaseous hydrogen, to contribute the development of recommended practices for material selection, safety operation and inspection intervals for hydrogen fuel station, the material testing on CrMo steels for gas cylinders under 45MPa gaseous hydrogen was extensively performed.

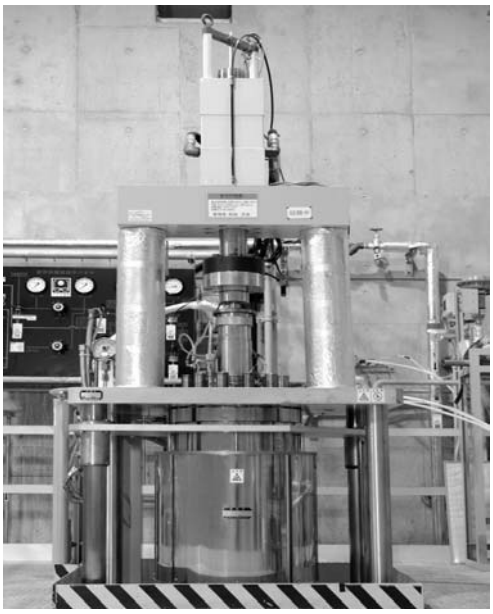

Figure 1 Hydraulic fatigue testing machine with 45MPa autoclave

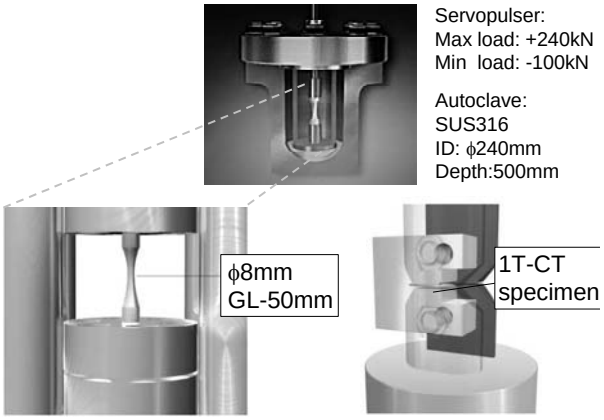

(a) Tensile test / Fatigue test (b) Crack growth test

Figure 2 Hydraulic fatigue testing machine with 45MPa autoclave

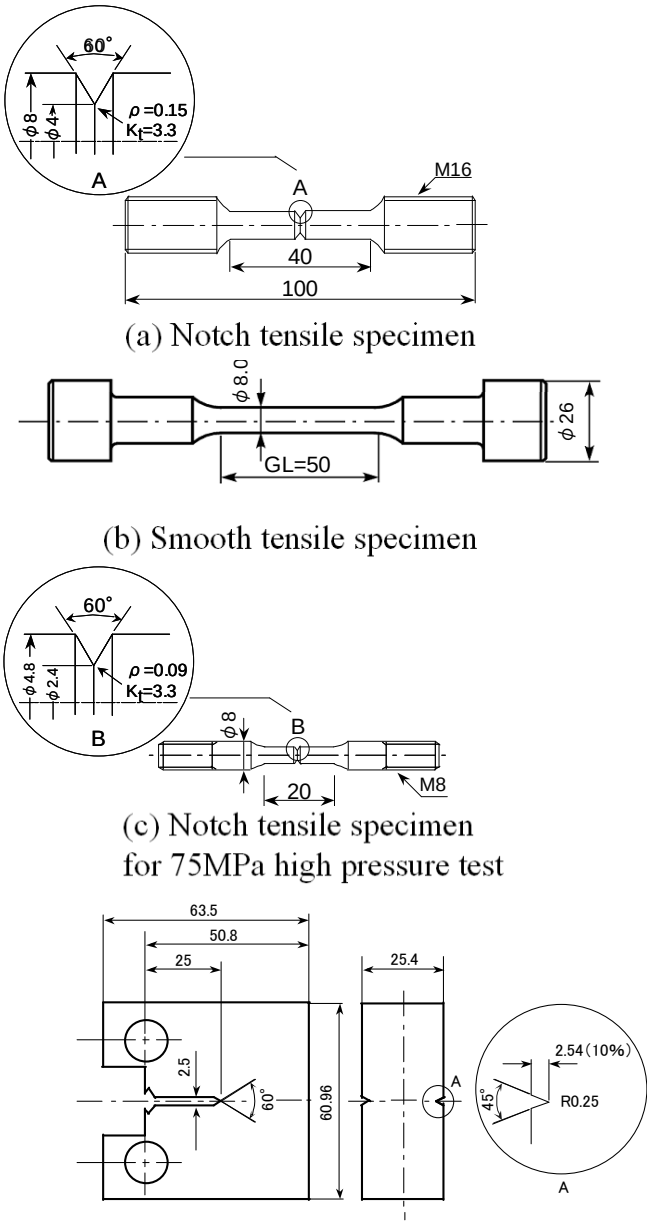

(a) Notch tensile specimen

(b) Smooth tensile specimen

(c) Notch tensile specimen for 75MPa high pressure test

(d) Crack growth specimen

Figure 3 Specimen geometry

2. EXPERIMENTAL

2.1 Test equipments

In order to perform such tensile test, hydraulic servo controlled testing machine with pressure vessel (Figure 1) was fabricated. The pressure vessel has an inside diameter of 240mm and the depth of 500mm. Figure 2 shows the appearance of specimen set in the autoclave test machine. The test machine was designed for round bar type specimen and compact specimen for crack growth testing. For crack growth testing, clip in displacement gage was mounted in crack mouth on the load line. For lower temperature test (-40°C, -20°C and 0°C), cryogenic chamber was set around autoclave. For higher temperature test (85°C), heater chamber was set around autoclave. Test temperature was controlled by thermocouple attached to the specimen.

Table 1 Chemical composition of the steel tested

Steel type, Steel / Chemical composition		Mass %								
		C	Si	Mn	P	S	Cu	Cr	Ni	Mo
SCM435	A	0.36	0.23	0.76	0.014	0.010	0.020	1.06	0.03	0.19
SCM440	B	0.42	0.22	0.76	0.008	0.003	0.02	1.10	0.02	0.24
	C	0.40	0.24	0.76	0.012	0.004	0.02	1.02	0.01	0.21
	D	0.42	0.23	0.77	0.012	0.0016	0.02	1.00	0.02	0.18

Table 2 Mechanical properties of as received steel tested in air

Steel		Thickness	Tensile test				Impact test
			T.S. (N/mm2)	0.2%Y.S. (N/mm2)	El. (%)	R.A. (%)	FATT (℃)
SCM435	A	35mm	958	781	19	58	+24
SCM440	B	16mm	1060	947	20	58	-
	C	70mm	979	773	19	54	+94
	D	28mm	1018	875	21	59	-66

Table 3 Tempering conditions for varying the tensile strength by laboratory heat treatment

Tempering Condition	Tensile Strength level (MPa)		
	SteelA'	Steel B'	SteelD'
400℃	1184	-	-
450℃	1071	-	-
500℃	1042	1340	1281
550℃	917	-	1135
600℃	824	1036	1003
650℃	-	935	879
700℃	-	816	765

Steel A' : Quench(850°C oilQ) and Tempering(WQ) the Steel A
Steel B' : Quench(855°C oilQ) and Tempering(WQ) the Steel B
Steel D' : Quench(855°C oilQ) and Tempering (WQ)the Steel D

2.2 Specimen Preparation

Figure 3 shows the specimens used in hydrogen mechanical testing. The surface of the smooth tensile specimen was prepared highly polished surface by abrasive paper (#800). For fracture toughness testing, compact tension specimens of 25.4mm thick (1T-CT) were pre-cracked in air.

2.3 Material

Test materials are commercial quenched & tempered SCM (JIS G 4105) low alloy series: SCM435 and SCM440 which are the popular materials for the high-pressure equipment. Chemical composition and mechanical properties are in Table 1 and Table 2. The SCM435 (steel A) was supplied from 35mm thick forged plate. SCM 440 steel B, C and D are 16mm, 70mm and 28mm in each thickness and all are rolled plate. For varying the tensile strength level, steel A, B and D were laboratory heat-treated and those are defined as steel A', B' and D' in order to distinguish from as received steels. The obtained tensile strengths are in Table3.

2.4 Environment

To minimize the experimental uncertainty caused by impurity gases, hydrogen gas used for material testing is 99.99999% purity by volume with the following impurity levels: O_2<0.02ppm, CO<0.01ppm with a dew point of − 80℃. Pressurization and system purging is conducted before testing: through (1) pressurization with dry N_2 gas, (2) evacuation and (3) pressurization/ depressurization with the pure hydrogen gas. Once, hydrogen gas pressure and specimen temperature were settled, test was set to start (i.e. no soaking time).

3. RESULTS AND DISCUSSIONS

3.1 Tensile properties

Figure 4 shows tensile curves in 20MPa gaseous hydrogen of steel A for various tensile strength levels. The tensile speed was 0.00015mm/sec in stroke speed in order for the strain rate nearly equal to be 10^{-5}/s. As strength level increases, the elongation in gaseous hydrogen decreases. It is noted that for the 1200MPa steel, the specimen fractured before it reaches maximum tensile strength level. This indicates that the 1200MPa steel does not have enough elongation capacity (i.e.: uniform elongation) that can withstand internal pressure bursting of a vessel. While 1000MPa steel fractured just after the specimen had started necking. The 800MPa steel seems almost no hydrogen gas effect on tensile properties.

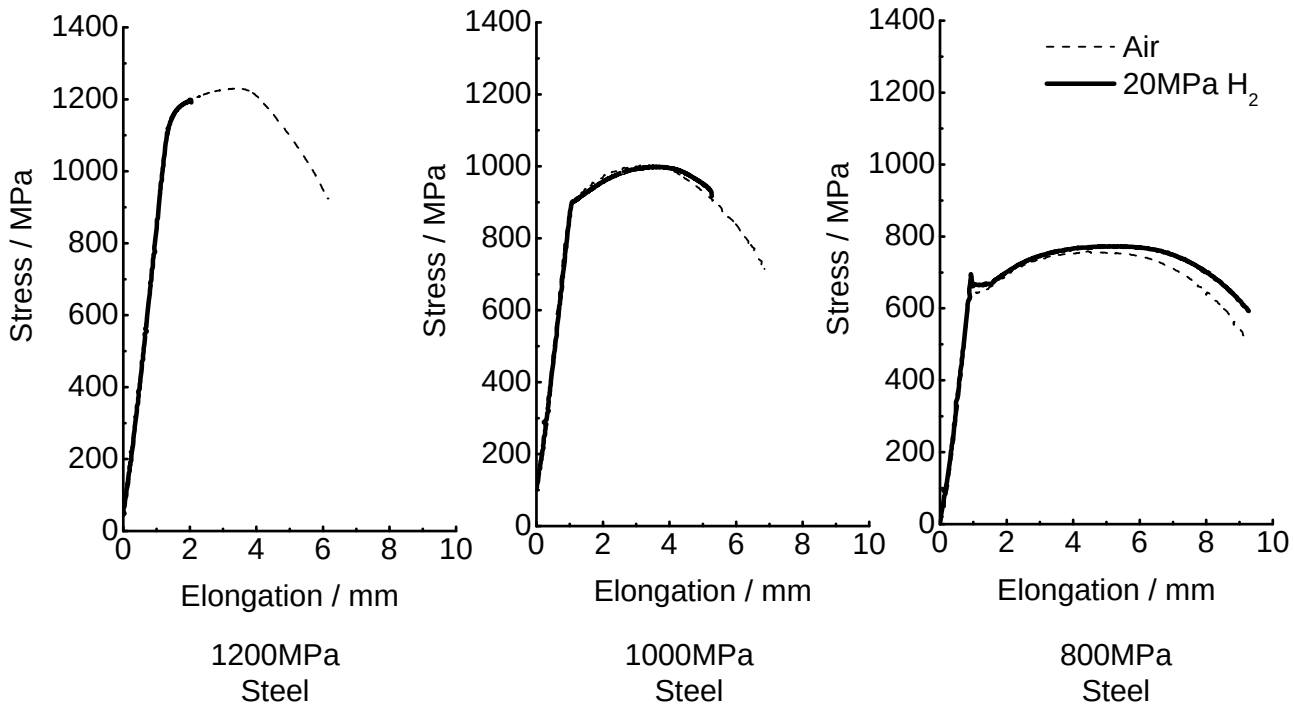

Figure 4 Load-displacement curves of steel A

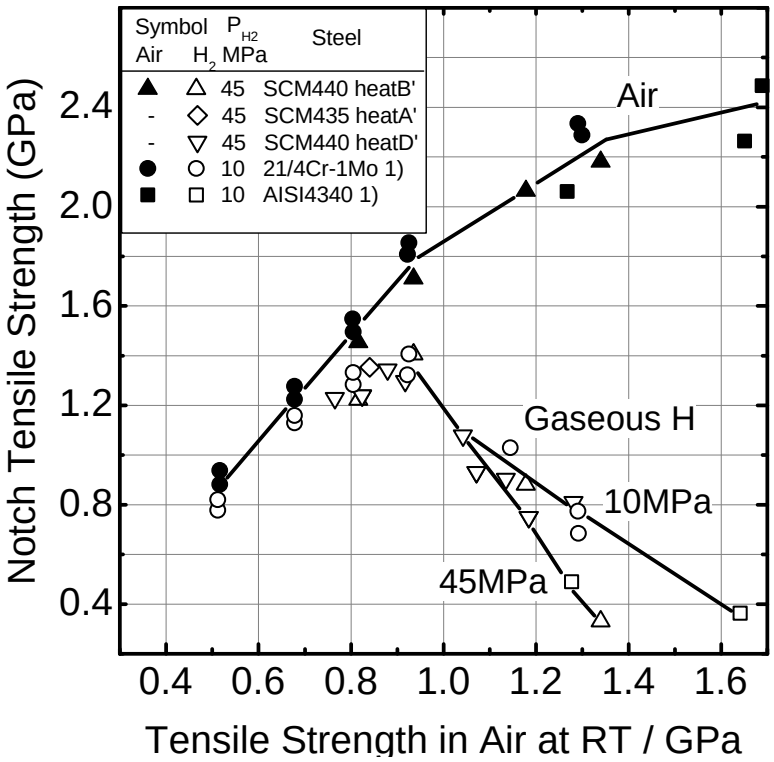

Figure 5 Notch tensile strength (NTS) as a function of steel tensile strengths

3.2 Effect of steel strength

Figure5 shows notch tensile strength (NTS) as a function of tensile strength of steel A', B' and D' plotted with the reference data **[1]**. The NTS in gaseous hydrogen substantially decreases above a tensile level of approximately 930MPa to 1000MPa, thus showing a maximum at this strength level. Our data in 45MPa pressure seem to show much more reduction in notch tensile strength at higher strength level than the data experimented under 10MPa pressure [1].

3.3 Effect of temperature

The tensile tests under -40 to 85°C ambient temperature were performed using the smooth tensile specimen.

For each temperature condition, the tests were conducted under both 45MPa hydrogen gas and 45MPa nitrogen gas respectively. In Figure 6, the elongation ratio (ξ_{H2}/ξ_{N2}) of the smooth tensile test specimen were plotted for steel A and steel D. The elongation ratio (ξ_{H2}/ξ_{N2}) itself of steel A and D is different to each other, though it is shown that the elongation reduction by the effect of hydrogen increased with lowering the temperature and at -40°C the hydrogen effect slightly increases. This trend is similar to the data reported by Hoffman and Rauls **[2]** evaluated on un-notched specimen of mild steel under the hydrogen pressure of 15.2MPa.

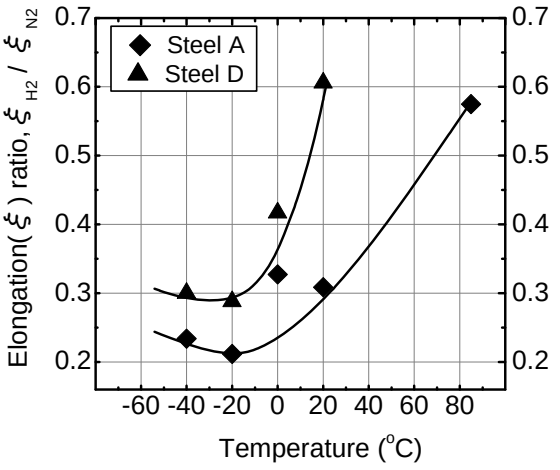

Figure 6 Effect of test temperature on elongation ratio (ξH2/ξN2) of the smooth tensile test specimen

3.4 Crack growth properties

3.4.1 Effect of hydrogen gas environment on fracture toughness

Crack growth tests in 45MPa gaseous hydrogen environment were performed using compact specimen (Fatigue pre cracking: Air, Specimen: 1.0T-CT). Figure 7 shows load displacement curves obtained under the loading rate (Load line displacement (δ) rate dδ/dt=0.005mm/s.). Steel D shows stable slow crack growth until the complete tearing of the specimen. On the other hand, steel C was fast fractured during the test. As is shown by the schematic drawing of the fractured surfaces of the specimen, it is clarified that fast fracture in steel C was

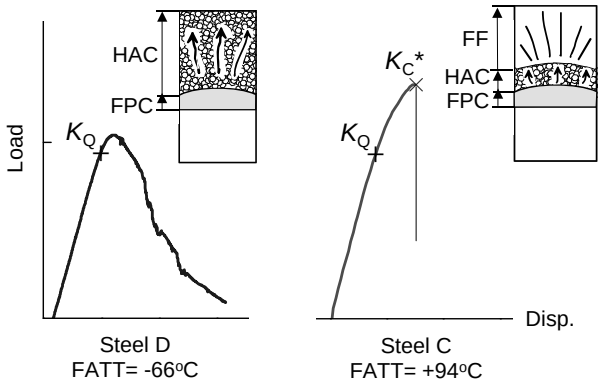

FPC: Fatigue Pre Crack, HAC: Hydrogen assisted Crack
FF: Fast Fracture

Figure 7 load displacement curves of crack growth test

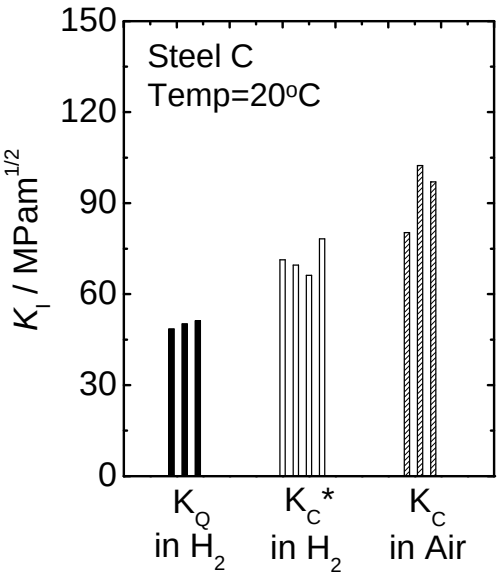

Figure 8 Fracture toughness K_C* by the final crack length and maximum load , fracture toughness K_C in air: and the stress intensity factor K_Q at the onset of cracking

occurred by cleavage fracture after the development of some 1 to 2millimeters stable H cracking. In Figure 8, K_Q (: stress intensity factor evaluated by the 5% secant line in load displacement curve, K_C*(: stress intensity factor at which fast fracture occurs, and K_C (: fracture toughness in air). From the fracture surface examinations, no crack blunting was observed at the boundary between fatigue pre-crack and extended crack in all specimens. Instead, quasi-cleavage fracture accompanied by inter-granular fracture, which were the characteristic fracture morphologies of hydrogen embrittlment, was observed. From those observation results, the loss of linearity on the load-displacement curves in Figure7 is attributed to the stable cracking by the effect of hydrogen environment embrittlment and K_Q represents the stress intensity factor at the onset of cracking. Also, there are no significant difference between K_C^* and K_C by the results of Figure8. Therefore, the gaseous hydrogen environment only affects the slow stable crack growth but did not affect the critical flaw growth of the steel at low temperature, i.e. fast fracture. The cause of low fracture toughness of steel C is attributed to the thickness (70mm) of material. That is, the steel has a brittle ferrite + bainite microstructure due to the insufficient cooling rate from austenitizing temperature.

3.4.2 Effect of temperature on crack growth behavior

Crack growth tests were conducted under -40 to 85°C ambient temperature. Loading rate and specimen condition are the same as described in 3.4.1. Figure 9 shows load-displacement curves of steel D. In all tests, fracture mode was governed by slow crack growth mode. It is obviously shown that there is a temperature dependence on load-displacement curve, where the extent of load drop caused by the slow crack growth development reaches maximum near 0°C. It should be recalled that elongation ratio (ξ_{H2}/ξ_{N2}) on smooth tensile specimen showed same sensitivity to temperature through the same range. Figure 10 shows load-displacement curves of steel

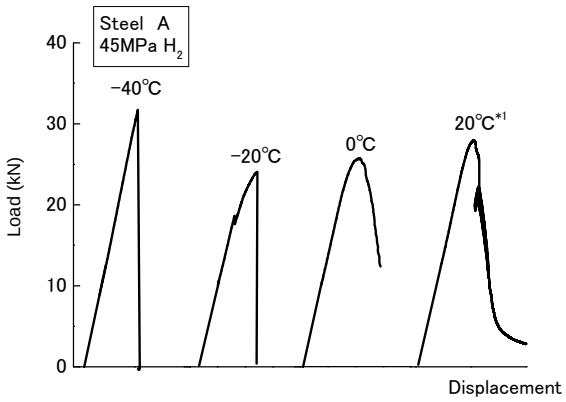

Figure 10 Load-displacement curve of steel A

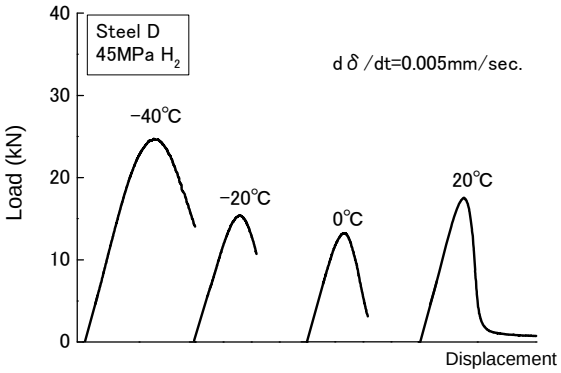

Figure 9 Load-displacement curve of steel D

A. The final fracture mode becomes to be dominated by the cleavage when the temperature falls below -20°C.

In Figure 11, K_Q in 45MPa hydrogen are plotted as a function of test temperature and comparison made with fracture toughness transition curve in air estimated from CVN data **[7]** of the steel D. It is understood from this figure that the fracture mode in gaseous hydrogen is dominated by slow crack growth (i.e.; no critical flaw growth) because of the upper shelf fracture toughness characteristics in all temperature range.

Figure 12 shows the same comparison made on steel A. It is explained by this figure that the cleavage fracture observed below -20°C tests in Figure 10 was occurred because the estimated ductile-to-brittle transition range of fracture toughness K_C lie in between -40°C to about +28°C.

The significance of those crack growth test results needs emphasizing that the steel's toughness for hydrogen pressure vessel has at least to have upper shelf characteristics at MDMT (Minimum Design Metal Temperature) to avoid critical failure

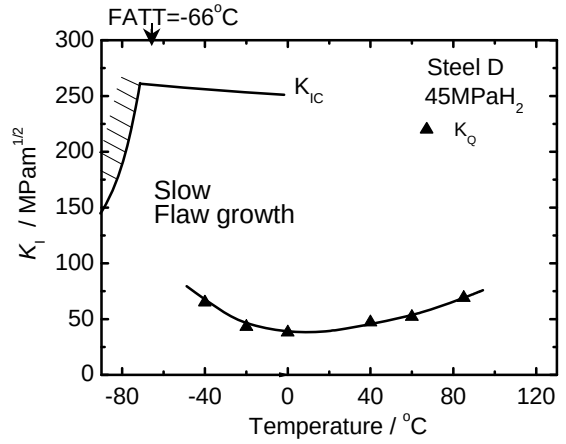

*1) : K_{IC} in Air was estimated from CVN curve

*2) : K_Q at 5% Secant line in load- displacement curv

Figure 11 K_Q and K_C as a function of test temperature for steel D

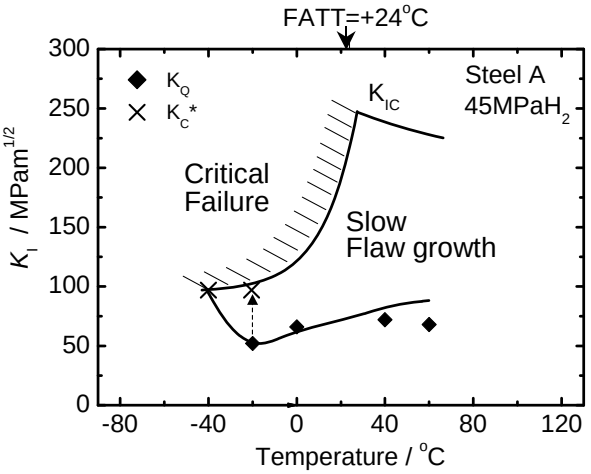

*1) : K_{IC} in Air was estimated from CVN curve

*2) : K_Q at 5% Secant line in load- displacement curve

3) : K_c at Fast Fracture

Figure 12 K_Q and K_C as a function of test temperature for steel A

events which would be triggered by the prior development of hydrogen crack extension. In practice, this can be qualified by obtaining Charpy V-notch curve.

.

3.5 Effect of 75MPa hydrogen pressure

Notch tensile test were performed using another 75MPa SSRT test machine. Due to the limitation of the capacity of the test equipment, the notch tensile specimen size is limited to smaller one as shown in Figure 3 than one as has already been introduced in 45MPa notch tensile test results. The effect of hydrogen pressure is shown in Figure13. The data scatter is large though, it can roughly be expressed by 1/2 power dependence upon an external hydrogen pressure.

Micro fractography were examined on those fractured specimen. Figure 14 shows whole fracture surfaces segmented by each fracture morphologies (Q: Quasi Cleavage, I: Inter-granular,C: Cleavage, M: Micro-void Coalescence). Figure 15 shows percentage of fracture mode obtained from the examination results of Figure 14. It is shown by those results that as the hydrogen pressure increases, the inter-granular fracture begins to take place with respect to micro void coalescence plus cleavage fracture. Figure 16 shows the detailed fracture observation by scanning electron microscopy. At lower pressure, the structure of fracture surface is characterized by quasi-cleavage and tear ridges (arrows in figure) are appreciable on cleavage facet, which indicate microscopic plastic flow during fracture. At higher pressure, the mixture mode of inter-granular fracture and quasi-cleavage

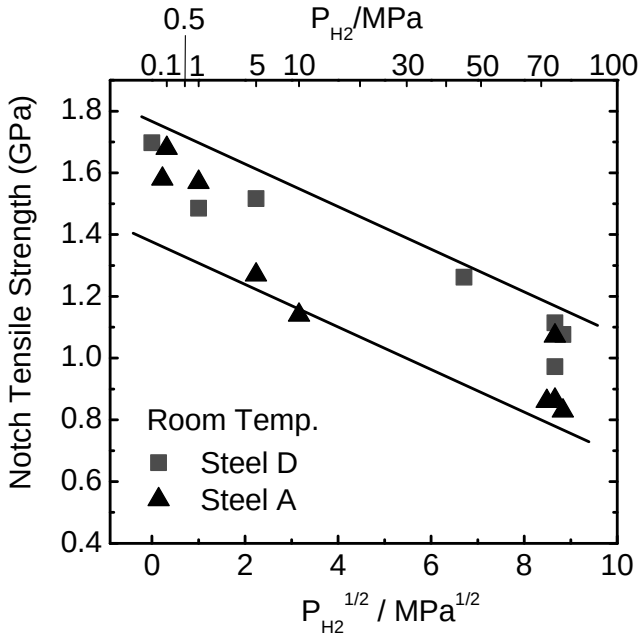

Figure 13 Effect of hydrogen pressure on Notch tensile strength

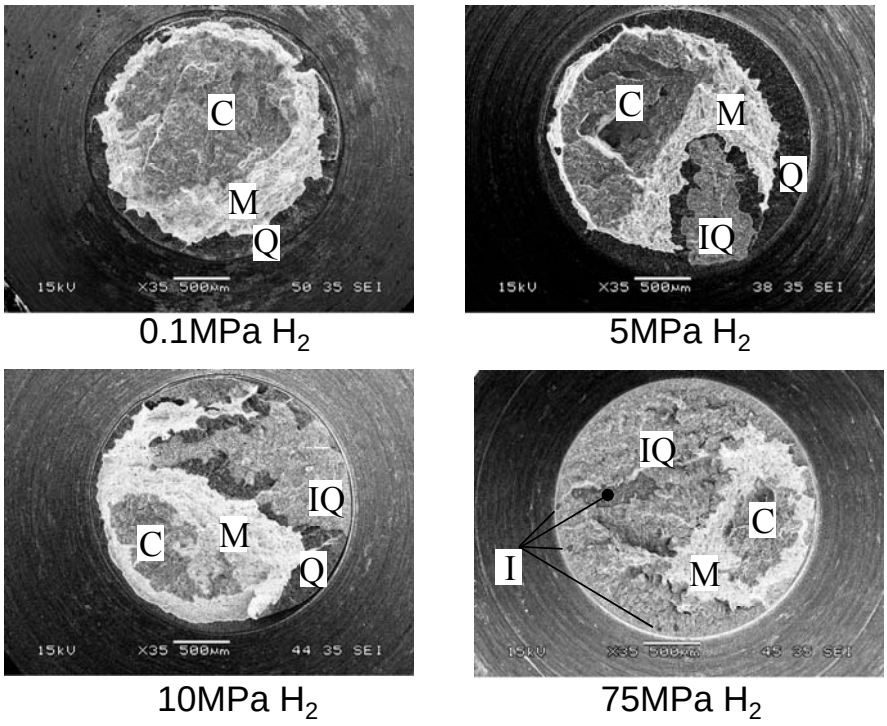

C:Cleavage
M:Micro Void Coalescene
Q:Quasi Cleavage
IQ: Intergranular + Quasi Cleavage
I: Intergranular

Figure 14 Micro fractography of the fractured specimen segmented by each fracture morphologies

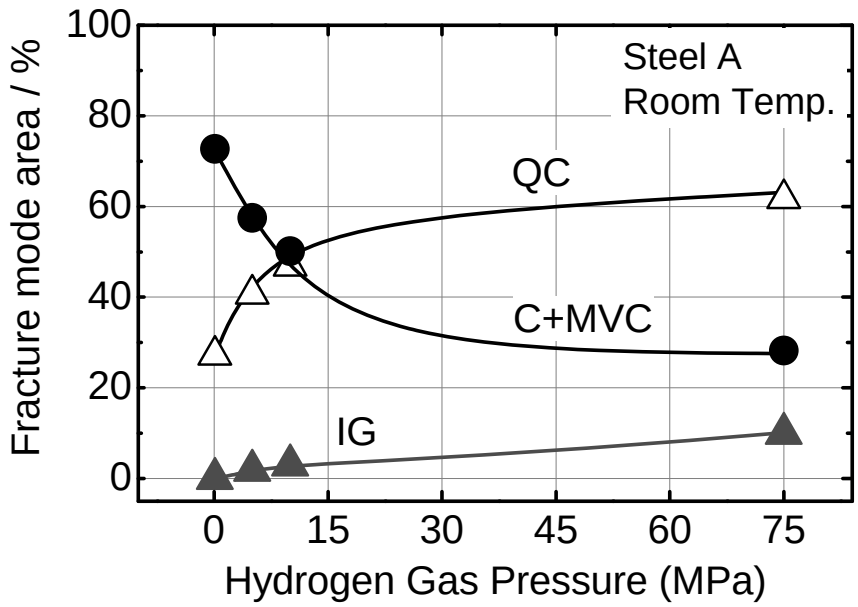

Figure 15 Percentage of fracture mode plotted as a function of pressure

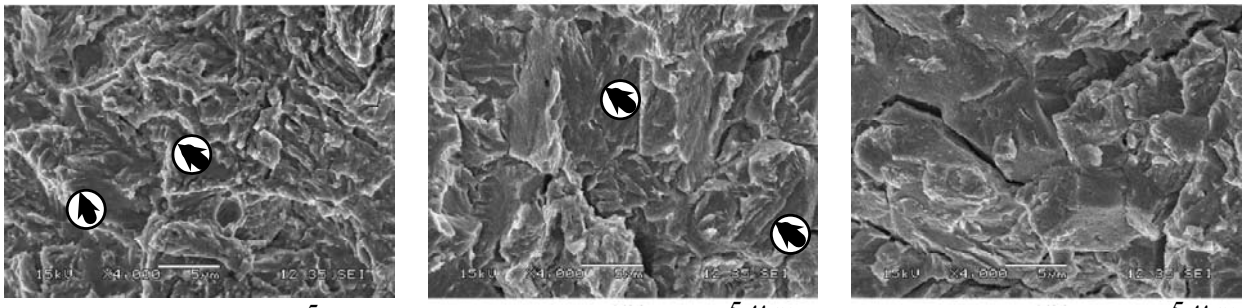

Figure 16 SEM observation of fractured surfaces

is predominant, where there are a number of secondary cracks existing along prior austenite grain boundaries. If it is assumed that the dissociation reaction $H_2 \rightarrow 2H$ is related to the external gas pressure, such that $C_0 \propto (\text{pressure})^{1/2}$. Solute concentration build up within the maximum hydrostatic stress field at the notch root also is about 27 times higher at 75MPa than the pressure at 0.1MPa as this basic idea and a model is proposed by Doig & Jones **[8]**. Therefore the enhancement of inter-granular cracking by pressure increase might be related to the hydrogen concentration at the notch root, which is explained by the 1/2 power dependence upon pressure.

SUMMARY CONCLUSIONS

The 1200MPa steel does not have enough elongation capacity (i.e.: uniform elongation) in hydrogen gas that can withstand internal pressure bursting of a vessel.

The NTS in gaseous hydrogen substantially decreases above a tensile level of approximately 930MPa to 1000MPa, thus showing a maximum at this strength level.

The elongation reduction by the effect of hydrogen increased with lowering the temperature and at -40°C the hydrogen effect slightly increases. The same sensitivity to temperature on crack growth behavior was observed.

It was shown that the gaseous hydrogen environment only affect the slow stable crack growth but did not affect the critical flaw growth of the steel at low temperature, i.e. fast fracture.

From above information, it should be mentioned that the steel's toughness for hydrogen pressure vessel has to at least have upper shelf characteristics at MDMT (Minimum Design Metal Temperature) to avoid critical failure events.

The pressure dependence of notch tensile strength ranging from 0.1MPa to 75MPa hydrogen pressure shows approximately 1/2 power dependence.

As the hydrogen pressure increases, the inter-granular fracture begins to take place. This enhancement of inter-granular cracking by pressure increase might be related to the hydrogen concentration at the notch root, which is explained by the 1/2 power dependence upon pressure.

ACKNOWLEDGEMENTS

This study is a part of "Research for safe technology about a hydrogen infrastructure" entrusted by New Energy and Industrial Technology Development Organization (NEDO) in Japan.

REFERENCES

1. Ohnishi, K., Chiba, R. and Ishizuka, J., Embrittlement of low alloy and austenitic steels under high pressure hydrogen gas at room temperature, Transaction of Japan Institute of Metals, Vol.21, p.485-488, 1980
2. Hofmann, W., and Rauls, W., Ductility of Steel Under the Influence of External High Pressure Hydrogen", Welding Journal, Vol.44-May, p.225s-230s, 1965
3. Nelson, H.G., Testing for Hydrogen Environment Embrittlement; Primary and Secondary Influences, Hydrogen Embrittlement Testing, ASTM STP543, 1974, p.152
4. Chandler, W.T. and Walter, R.J., Testing to Determine the Effect of High Pressure Hydrogen Environments on the Mechanical Properties of Metals, ASTM STP543, 1974, p.170-197
5. Gray, H.R., Testing for Hydrogen Environment Embrittlement: Experimental Variables, Hydrogen Embrittlement Testing, ASTM STP543, 1974, p.133-1513
6. Fukuyama.S, Yokogawa.K and Araki.K, Fracture Toughness And Fatigue Crack Growth Of AISI4340 Steel In High Pressure Hydrogen At Room Temperature, Pressure Vessel Technology, Vol.2, 1989 , p.1181-1188
7. Iwadate T, Karaushi T, Watanabe J, , Fracture Toughness Of Temper embrittled 21/4Cr-1Mo and 3.5 Ni-Cr-Mo-V Steels, Pressure Vessel Technology, Vol.2, 1989 , p.1181-1188
8. Doig.P. and Jones G.T., A Model For the Initiation of Hydrogen Embrittlment Cracking at Notches in Gaseous Hydrogen Environments, Metallugical Transactions A, Vol8A, 1977, p.1993-1997